A Micromechanical Model for Wave Propagation in Plain-Weave Textile Composites

Wael G. Abdelrahman[1]
King Fahd University of Petroleum and Minerals, Dhahran, Saudi Arabia, 31261

[Abstract] In this paper we adapt and extend the results of a recently developed continuum mixture model to study wave propagation interaction with plain weave textile composites. The original model, which was first used to study wave propagation in bi-laminated composites, is based on approximate distributions for some of the transverse stress and displacement components. This results in two coupled partial differential equations describing the micromechanical behavior of the layered composite. Next, we idealize the complex weave unit cell into segments of bi-laminated composite, which geometrically model the undulation. Formal solutions for the two coupled equations are then obtained in each of the segments. Finally, the transfer matrix method is used to relate the solutions at one end of the idealized unit cell to the other, to obtain the unit cell global transfer matrix and to derive the dispersion equation of the system. The procedure is applied to a graphite-epoxy plain-weave composite and several characteristics are observed. Very good convergence is achieved using only a small number of segments.

Nomenclature

A	=	transfer matrix of a composite segment
a	=	length of the straight part of the idealized unit cell
b	=	length of the tapered part of the idealized unit cell
C	=	stiffness matrix of the weave tow
c	=	wave speed
d	=	half minimum height of the idealized unit cell
h	=	half thickness of the yarn
L	=	length of the idealized unit cell
n	=	number of segments in tapered part
n_1	=	volume fraction of weft
n_2	=	volume fraction of warp
t	=	time
U	=	displacement amplitude
u	=	displacement vector
V	=	displacement amplitude ratio
α	=	characteristic value
ρ	=	density of the weave material
σ	=	stress tensor
ω	=	angular frequency of the propagating wave
ξ	=	wave number

I. Introduction

Textile Composites in general, and plain-weave fabrics in particular, proved to be complex, structural materials with the potential of enhancing many of the shortcomings of conventional layered or fiber-reinforced composites. Plain-weave composites consist of two sets of interlaced fibers, known as the warp and the weft tows.

[1] Assistant Professor, Department of Aerospace Engineering, Mail Stop 1694.

Figure 1a illustrates a repeating unit cell of such a composite. Often, the system is coated with a resin material added to the warp and the weft and hence such added material plays the role of the matrix.

The mechanics of plain-weave composites are set apart from that of straight fibrous composites by several complicating factors. The first is concerned with its large relaxing initial deformation effects.[1] The second is concerned with their complicated geometric morphology. This is mainly due to the nature of undulation of the warp and weft components, the kinking and also to the resulting inherent periodicity. To assess plain weave utility in structural applications, an understanding of their micromechanical behavior is required. As a minimum, their effective anisotropic properties need to be calculated. Also micro-structural information regarding the degree of interaction between the warp and weft components is of prime importance if damage assessment is of concern.

Several approximate model analyses aimed at deriving effective properties of plain-weave composites are readily available. Most of these models are based on static loading analysis.[2-5] Comparatively speaking, very little work is available that deals with their micro-structural behavior especially under dynamic loading. Most of the work in the literature is based on experimental measurements or deal with the propagation of Lamb waves. Stempien[6] developed a method for estimating the tension wave propagation velocity in flat textile composites by means of an optoelectronic transducer. Tasdemirci et al.[7] studied the effects of stress wave propagation in S2 glass woven fibers with SC15 epoxy composite plates. Later Tasdemirci and Hall[8] combined experimental techniques and numerical modeling to investigate the severe stress discontinuities in multilayered woven composites. The study of harmonic wave propagation along an axis of symmetry in such materials adds to the understanding of their micro-structural behavior. The aim of this present work is to present such a study.

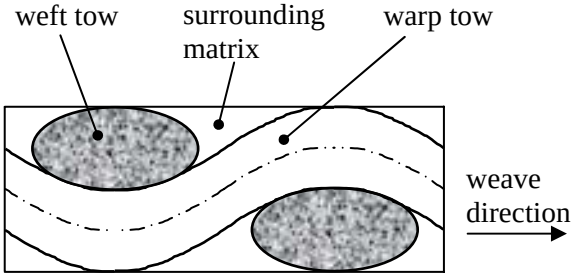

a) Repeating unit cell of the plain weave textile

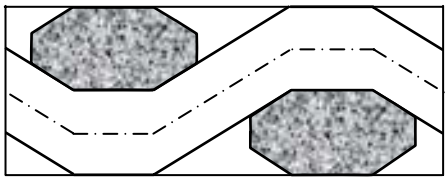

b) First step idealization: the warp undulation

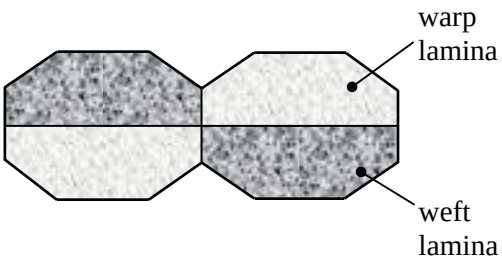

c) Second step idealization: the variable thickness mosaic model

Figure 1. Geometric idealization of the textile.

The complicated geometry of Fig. 1a suggests that exact solutions are not possible to obtain. As an alternative, we seek approximate modeling based on some idealization of the cell geometry. Figure 1b presents an idealization of that of Fig. 1a. It smoothes the undulation and presents instead an inclined segment in the warp component. Even here, the geometry is still difficult to handle. By adopting the mosaic type model of Fig. 1c, we get a representative geometry that can be handled with relative ease. Besides its relative analytic tractability, it includes an attractive feature concerning the symmetry of the warp and weft layering. Here, we are also assured of retaining an element of undulation and the inherent periodicity of the system. Missing however is the bonding material of the system, which we are also neglecting for simplicity. Furthermore, the system is periodic along the propagation direction and is expected to lead to Bloch-type waves.

II. Analysis of the Bi-layered System

To illustrate the model, we now consider the bi-layered system shown in Fig. 2. The behavior of this system is described by the field equations that hold for both components 1 and 2, respectively:

$$\frac{\partial \sigma_x}{\partial x} + \frac{\partial \sigma_{xy}}{\partial y} = \rho \frac{\partial^2 u_x}{\partial t^2} \tag{1}$$

$$\frac{\partial \sigma_{xy}}{\partial x} + \frac{\partial \sigma_y}{\partial y} = \rho \frac{\partial^2 u_y}{\partial t^2} \tag{2}$$

and the constitutive relations:

$$\sigma_x = C_{11} \frac{\partial u_x}{\partial x} + C_{12} \frac{\partial u_y}{\partial y} \tag{3}$$

$$\sigma_y = C_{12} \frac{\partial u_x}{\partial x} + C_{22} \frac{\partial u_y}{\partial y} \tag{4}$$

$$\sigma_{xy} = C_{66} \frac{\partial u_x}{\partial y} \tag{5}$$

These equations are supplemented with the appropriate symmetry and continuity conditions shown in Fig. 2.

Rather than solving the field equations for each lamina subject to satisfying all boundary and interface conditions, a rational construction of an alternative set of coupled equations that automatically satisfy all interface conditions is presented. This leads to simple coupled governing equations for the total composite which retain the integrity of each component but allow them to coexist under some derived interfacial transfer terms. Here, information on the distribution of displacements and stresses within each component are readily available. The construction procedure is inevitably based on some approximating assumptions. These are mainly concerned with the introduction of through-thickness approximate distributions for some of the field variables, which automatically satisfy symmetry and interface conditions. Similar approximations were presented in our previous application of the proposed technique to the concentric cylindrical model.[9] Confidence in our modeling was gained by good comparisons to experimental data.

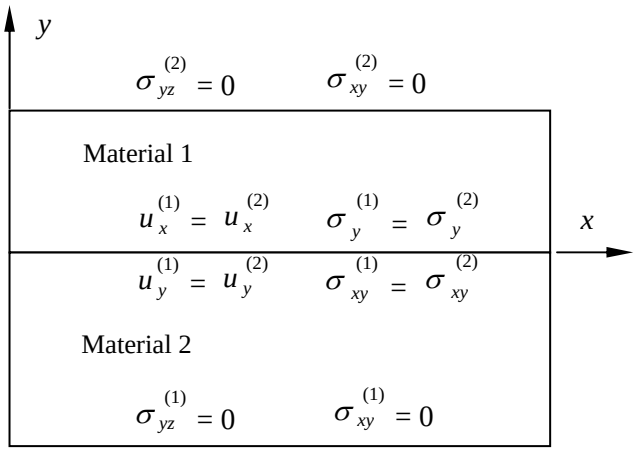

Figure 2. Symmetry and continuity conditions of the bi-laminated model.

For the laminated problem at hand, we follow the same approach we used for the concentric cylinder model. Once again, we use the averaging technique as a means to facilitate our analysis and to manipulate some of the algebraic expressions. In no where we find it necessary to satisfy any required equation, boundary or interface condition based on its average. Details of the procedure used here are readily available in Ref. 9.

For the present improved mosaic model the field equations, Eqs. (1) and (2), are combined with the constitutive relations (3-5), to yield the two coupled equations

$$a_{11} \frac{\partial^2 u_x^{(1)}}{\partial x^2} + a_{12} \frac{\partial^2 u_x^{(2)}}{\partial x^2} + \frac{n_1}{\eta_2} \left(u_x^{(2)} - u_x^{(1)} \right) = n_1 \rho_1 \frac{\partial^2 u_x^{(1)}}{\partial t^2} \tag{6}$$

$$a_{22}\frac{\partial^2 u_x^{(2)}}{\partial x^2} - a_{21}\frac{\partial^2 u_x^{(1)}}{\partial x^2} - \frac{n_1}{\eta_2}\left(u_x^{(2)} - u_x^{(1)}\right) = n_2\rho_2\frac{\partial^2 u_x^{(2)}}{\partial t^2} \tag{7}$$

where

$$\eta_2 = \frac{n_1 h_i^{\,2}}{3}\left(\frac{n_1}{C_{66}^{(1)}} + \frac{n_2}{C_{66}^{(2)}}\right) \tag{8}$$

and where

$$a_{11} = n_1 C_{11}^{(1)} + n_2 C_{12}^{(1)} C_{66}^{(1)} F \tag{9}$$

$$a_{12} = n_1 C_{12}^{(1)} C_{66}^{(2)} F \tag{10}$$

$$a_{21} = -n_2 C_{12}^{(2)} C_{66}^{(1)} F \tag{11}$$

$$a_{22} = n_2 C_{11}^{(2)} - n_1 C_{12}^{(2)} C_{66}^{(2)} F \tag{12}$$

with F and D being defined as

$$F = \frac{C_{12}^{(2)} - C_{12}^{(1)}}{D\,(n_1 C_{66}^{(2)} + n_2 C_{66}^{(1)})} \tag{13}$$

$$D = \frac{1}{n_1 n_2}(n_1 C_{22}^{(2)} + n_2 C_{22}^{(1)}) \tag{14}$$

These equations are valid for any bi-laminated segment i with uniform total thickness $2h_i$. We now adopt the above model to describe the behavior of each of the mosaic segments. Since the straight segments have uniform thickness constituents, Eqs. (6) and (7) can be directly applied to them. And we see now that if we obtain formal solutions for one segment, then solutions for the second straight segment can merely be obtained by interchanging the role of both constituents. To maintain reasonable uniform thickness of the constituents, we shall approximate each of the inclined segments by a number n of sub-segments. Obviously, the layered model is also applicable to each of them. We recognize that the unit cell will consist of $4n+2$ sub-segments (see Fig. 3).

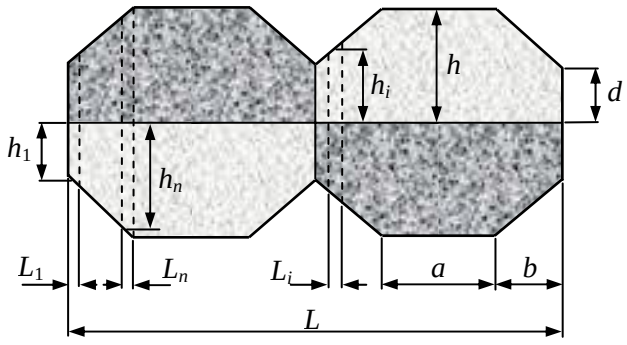

Figure 3. Geometry discretization of the idealized unit cell.

The half thickness of the ith sub-segment, h_i, is calculated from

$$h_i = h - \frac{(2i-1)(h-d)}{2n} \tag{15}$$

If we are able to find formal solutions in each of these sub-segments, then the transfer matrix method will be ideal for constructing the behavior of the total system. This method, which is described in details in Nayfeh[10], requires expressing the formal solutions in each sub-segment in terms of wave amplitudes. Eliminating these amplitudes relates the displacements and stresses on one side of each sub-segment to those on the other. By subsequently satisfying appropriate continuity conditions at the interfaces, we construct a global transfer matrix, which relates the displacements on one side of the total unit cell to those on the other.

III. Formal Solutions

For a plane wave propagating along the direction of layering, the formal solutions for the displacements $u_x^{(1)}$ and $u_x^{(2)}$ are given in Nayfeh[10] as:

$$(u_x^{(1)}, u_z^{(2)}) = (U_1, U_2)\, e^{i\xi(\alpha x - ct)} \tag{16}$$

where α is an unknown parameter and the longitudinal wave number $\xi = \omega / c$.

Substituting this solution into Eqs. (6) and (7) yields a set of two linear homogeneous equations in the amplitudes. In matrix form, the two-coupled equations are

$$\begin{bmatrix} n_1\rho_1\omega^2 - a_{11}\xi^2\alpha^2 - \dfrac{n_1}{\eta_2} & -a_{12}\xi^2\alpha^2 + \dfrac{n_1}{\eta_2} \\ a_{21}\xi^2\alpha^2 + \dfrac{n_1}{\eta_2} & n_2\rho_2\omega^2 - a_{22}\xi^2\alpha^2 - \dfrac{n_1}{\eta_2} \end{bmatrix} \begin{Bmatrix} U_1 \\ U_2 \end{Bmatrix} = \underline{0} \tag{17}$$

For nonzero solution of the amplitudes, the determinant of this equation must be equal to zero. This yields a fourth order polynomial relating α to the phase velocity c. Solutions for α occur in two pairs. Each pair consists of two values that are equal in magnitude but opposite in sign to each other. Corresponding to each α_q, q= 1, 2, 3, 4, Eq. (17) yields the amplitude ratio $V_q = U_{2q} / U_{1q}$ as

$$V_q = \frac{-(n_1\rho_1\omega^2 - a_{11}\xi^2\alpha_q{}^2 - n_1/\eta_2)}{-a_{12}\,\xi\alpha_q + n_1/\eta_2} \tag{18}$$

Using the principle of superposition, together with the constitutive relation (3), the formal solution for the relevant displacements and stresses take the form:

$$(u_x^{(1)}, u_x^{(2)}) = \sum_{q=1}^{4} (1, V_q)\, e^{i\xi(\alpha x + -ct)} \tag{19}$$

$$(\sigma_x^{(1)}, \sigma_x^{(2)}) = \sum_{q=1}^{4} i\xi (D_{1q}, D_{2q})\, e^{i\xi(\alpha x - ct)} \tag{20}$$

where

$$D_{1q} = (C_{11}^{(1)} + n_2/n_1 F C_{12}^{(1)} C_{66}^{(1)})\xi\alpha_q + (F C_{12}^{(1)} C_{66}^{(2)}) V_q \alpha_q \tag{21}$$

and

$$D_{2q} = (C_{11}^{(2)} - n_2 / n_1 FC_{12}^{(2)} C_{66}^{(2)}) V_q \alpha_q - (FC_{12}^{(2)} C_{66}^{(1)}) \alpha_q \tag{22}$$

Following the procedure described in Nayfeh[10], in the case of multi-segmented composite, we specialize the formal solutions to the right and left faces of each sub-segment and combine the resulting equations to get

$$P_i^+ = A_i P_i^- \tag{23}$$

where i = 1, 2,… $4n$+2. Here A_i is the transfer matrix for the sub-segment i, given by

$$A_i = X_i D_i^+ X_i^{-1} \tag{24}$$

and P_i is the vector of unknown displacements and stress resultants

$$P_i = \begin{bmatrix} u_x^{(1)} & u_x^{(2)} & F_x^{(1)} & F_x^{(2)} \end{bmatrix} \tag{25}$$

with the stress resultant given by

$$F_x^{(j)} = \sigma_x^{(j)} h_i \tag{26}$$

In Eq. (24), the matrix of coefficients X_i is given by:

$$X_i = \begin{bmatrix} 1 & 1 & 1 & 1 \\ V_1 & V_1 & V_2 & V_2 \\ D_{11} h_i & -D_{11} h_i & D_{12} h_i & -D_{12} h_i \\ D_{21} h_i & -D_{21} h_i & D_{22} h_i & -D_{22} h_i \end{bmatrix} \tag{27}$$

and the diagonal matrix of the system is:

$$D_i^+ = \begin{bmatrix} e^{i\xi\alpha_1 h_i} & & & \\ & e^{-i\xi\alpha_1 h_i} & & \\ & & e^{i\xi\alpha_2 h_i} & \\ & & & e^{-i\xi\alpha_2 h_i} \end{bmatrix} \tag{28}$$

Continuity between two adjacent sub-segments implies that

$$P_i^+ = P_{i+1}^- \tag{29}$$

where i = 1, 2, ...$4n$+2. This equation, when combined with Eq. (23), leads to:

$$P_{4n+2}^+ = A P_1^- \tag{30}$$

where

$$A = A_{4n+2} A_{4n+1} \ldots A_2 A_1 \tag{31}$$

is the global transfer matrix for the multi-segmented composite system (i.e. for the complete unit cell.) Periodicity of the composite system along the direction of wave propagation requires that

$$P_{4n+2}^+ = P_1^- e^{i\xi L} \tag{32}$$

Finally, we combine Eqs. (30) and (32) to obtain the dispersion characteristic equation

$$\left| A - e^{i\xi L} \right| = 0 \tag{33}$$

relating the phase velocity c to the wave number ξ. This equation does not have solution for all frequency values. Rather, the frequency range is divided into bands of allowed and forbidden frequencies, corresponding to real and imaginary $e^{i\xi L}$, respectively. These can be found from Eq. (33) by setting $\xi L = 2n\pi$, and solving for the frequency.

IV. Numerical Illustration and Discussion

As an illustration of the proposed modeling, we consider the case of wave propagation in a graphite-epoxy woven composite. With reference to Fig. 3, the unit cell has the following dimensions: h=0.2 cm, a/h=1, b/h=1.5, d/h=0.5. The transversely isotropic weave and weft tows have the same fiber volume fraction of 0.5. The stiffness matrix of the weave tow is calculated as: C_{11}=157, C_{12}=C_{13}=4.659, C_{23}=4.29, C_{44}=3.33, C_{55}=C_{66}=7.47 GPa. The stiffness matrix of the weft is obtained by interchanging 1 and 2 in C_{ij}. The density of the tow is $\rho = 1.6$ gm/cm^3.

Figure 4 shows the convergence characteristics of the solution. The value of the zero frequency limit of the wave speed asymptotically reaches its correct value with increasing number of segments. The monotonic convergence is so fast that with only 3 segments, the error is less than 1%. For the following illustrations, this value of n=3 is chosen.

Figures 5 and 6 show the dispersion characteristics of the composite unit cell. As Fig. 6

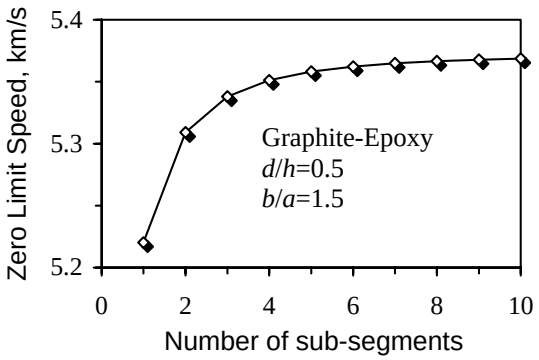

Figure 4. Convergence of the zero-limit wave speed with number of inclined segments *n*.

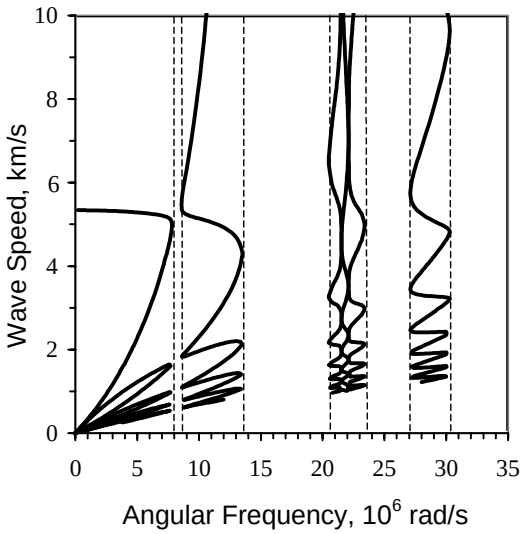

Figure 5. Dispersion curves for the first five modes for a graphite-epoxy plain weave.

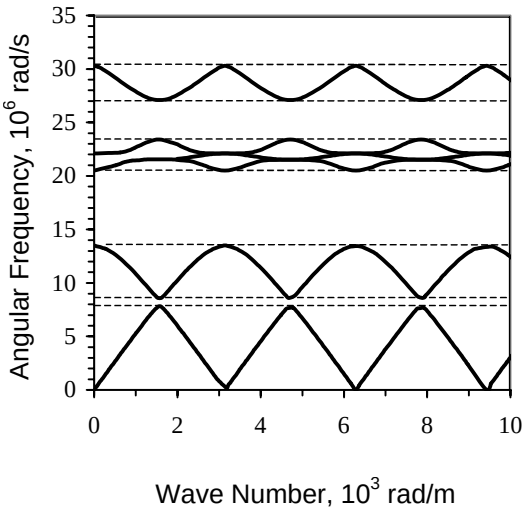

Figure 6. Dispersion curves of the illustration showing the frequency stop bands.

indicates, the curves have either a maximum or a minimum at wave numbers equal to multiples of π and $\pi/2$. Figures 5 and 6 clearly demonstrate the existence of a band structure with its allowed and forbidden frequencies.

Finally, we study the effect of the undulation angle on the analysis results. Amount of undulation can be expressed by the ratio d/h. Figure 7 shows the variation of the zero frequency limit of the wave speed with increasing values of d/h. As the figure demonstrates, the variation is almost linear. Increasing the undulation of the woven composite, which means decreasing d/h ratio, significantly increases the wave speed.

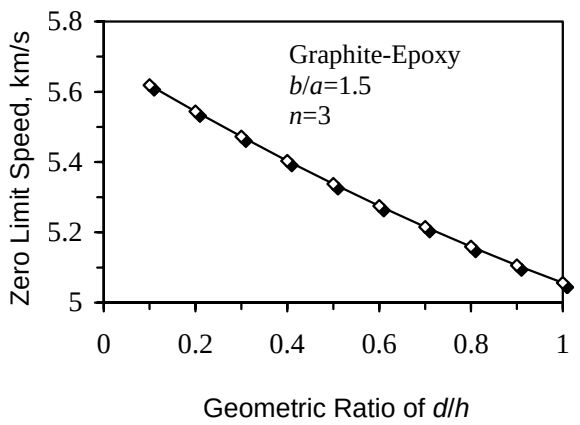

Figure 7. Effect of fiber undulation on the zero-limit wave speed in graphite-epoxy textile.

V. Conclusion

In this paper the different characteristics of wave propagation in plain weave textiles has been investigated. A previously developed model has been applied to an idealized unit cell of the textile composite. The transfer matrix method, combined with formal solutions of the resulting system of differential equations, is proved to be ideal for constructing the behavior of the total system. The dispersion equation of the system has been used to study the variation of the zero frequency limit of the wave speed with various values of the textile undulation. Several stop bands are shown to exist in the dispersion curves of graphite-epoxy textiles. It is concluded that undulation significantly increases the wave speed. The model shows potential for application in other classes of problems, including wave propagation in three-layered textile composites, and forced oscillations of woven composites.

Acknowledgments

The author is grateful to King Fahd University of Petroleum and Minerals for its support to this work.

References

[1]Nayfeh, A. H. and Kress, G. R., "Non-linear Constitutive Model for Plain-Weave Composites," *Composites Part B: Engineering*, Vol. 28, No. 5, 1997, pp. 627-634.

[2]Pandey, R. and Hahn, H. T., "A Micromechanics Model for 2D Fabrics," *37th AIAA/ASME/ASCE/AHS/ASC Structures, Structural Dynamics and Materials Conference*, AIAA, Washington, DC, 1996, pp. 359-368.

[3]Pochiraju, K., Chou, T-W, and Shah B. M., "Modeling Stiffness and Strength of 3-D Textile Structural Composites," *37th AIAA/ASME/ASCE/AHS/ASC Structures, Structural Dynamics and Materials Conference*, AIAA, Washington, DC, 1996, pp. 2294-2304.

[4]Whitcomb, J. and Tang, X., "Effective Moduli of Woven Composites", *Journal of Composite Materials*, Vol. 35, No. 23, 2001, pp. 2127-2144.

[5]Zeman, J. and Sejnoha, M., "Homogenization of Balanced Plain Weave Composites with Imperfect Microstructure: Part I-Theoretical Formulation", *International Journal of Solids and Structures*, Vol. 41, No. 22-23, 2004, pp. 6549-6571.

[6]Stempien, Z., "Method of Estimation of the Tension Wave Propagation in Flat Textile Products," *Fibres & Textiles in Eastern Europe*, Vol. 12, No. 3, 2004, pp.43-47.

[7] Tasdemirci, A., Hall, I. W., Gama, B. A., and Guden, M., "Stress Wave Propagation Effects in Two- and Three-layered Composite Materials," *Journal of Composite Materials*, Vol. 38, No. 12, 2004, pp. 995-1009.

[8]Tasdemirci, A. and Hall, I. W., "Experimental and Modeling Studies of Stress Wave Propagation in Multilayer Composite Materials: Low Modulus Interlayer Effects," *Journal of Composite Materials*, Vol. 39, No. 11, 2005, pp. 981-1005.

[9]Nayfeh, A. H. and Abdelrahman, W. G., "An Improved Continuum Mixture Model for Wave Propagation in Fibrous Composites," *Journal of the Acoustical Society of America*, Vol. 104, No. 2, 1998, pp. 867-873.

[10]Nayfeh, A. H., Wave Propagation in Layered Anisotropic Media with Application to Composites, Elsevier Publishing Co., Amsterdam, 1995.